Article

Cell Stem Cell

An *Apela* RNA-Containing Negative Feedback Loop Regulates p53-Mediated Apoptosis in Embryonic Stem Cells

Graphical Abstract

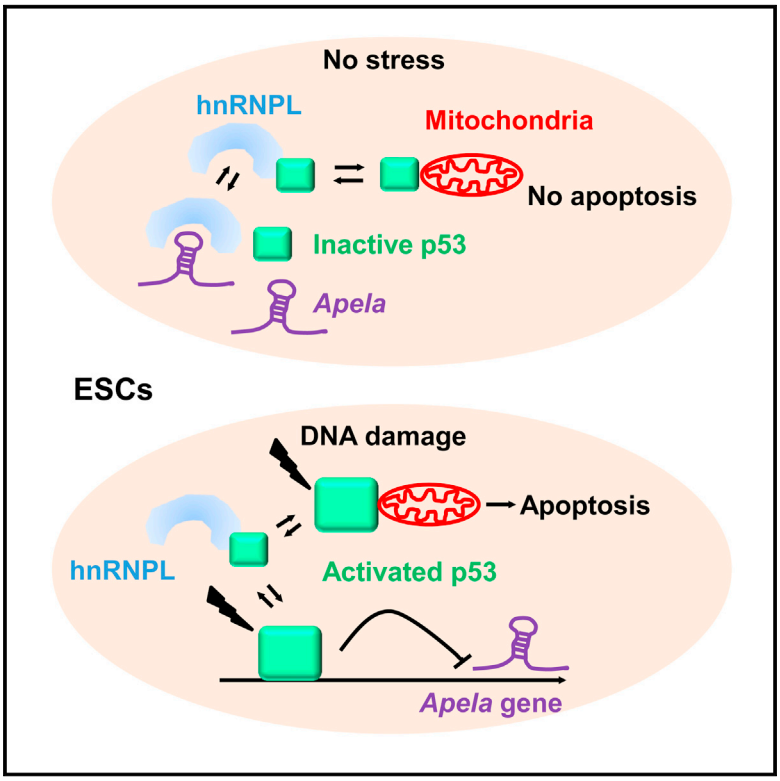

Authors

Mangmang Li, Hongfeng Gou, ..., Ming Zhou, Jing Huang

Correspondence

huangj3@mail.nih.gov

In Brief

Li et al. show that an ESC-enriched regulatory RNA, *Apela*, positively regulates p53-mediated DNA damage-induced apoptosis (DIA) of ESCs. *Apela*, hnRNPL, and p53 form a tri-element negative feedback loop that may help ESCs navigate the balance between maintaining inactive p53 under baseline conditions and eliciting DIA upon DNA damage.

Highlights

- *Apela* is enriched in mouse ESCs and repressed by p53
- *Apela* positively regulates DNA damage-induced apoptosis in mouse ESCs
- The protein-coding capacity of *Apela* is not required for DNA damage-induced apoptosis
- *Apela* binds to hnRNPL, an inhibitory binding partner of p53 in mouse ESCs

Accession Numbers

GSE65491

Li et al., 2015, Cell Stem Cell *16*, 669–683
June 4, 2015
http://dx.doi.org/10.1016/j.stem.2015.04.002

CellPress

Cell Stem Cell
Article

An *Apela* RNA-Containing Negative Feedback Loop Regulates p53-Mediated Apoptosis in Embryonic Stem Cells

Mangmang Li,[1,6] Hongfeng Gou,[1,6] Brajendra K. Tripathi,[2] Jing Huang,[3] Shunlin Jiang,[1] Wendy Dubois,[1] Tim Waybright,[4] Ming Lei,[3] Jianxin Shi,[5] Ming Zhou,[4] and Jing Huang[1,*]
[1]Cancer and Stem Cell Epigenetics, Laboratory of Cancer Biology and Genetics, Center for Cancer Research, National Cancer Institute, Bethesda, MD 20892, USA
[2]Signaling and Oncogenesis Section, Laboratory of Cellular Oncology, Center for Cancer Research, National Cancer Institute, Bethesda, MD 20892, USA
[3]Howard Hughes Medical Institute, Department of Biological Chemistry, University of Michigan, 1150 West Medical Center Drive MSRB3, 3315, Ann Arbor, MI 48109, USA
[4]Protein Characterization Laboratory, Cancer Research Technology Program, Frederick National Laboratory for Cancer Research, P.O. Box B, Frederick, MD 21702, USA
[5]Biostatistics Branch, Division of Cancer Epidemiology and Genetics, National Cancer Institute, Executive Plaza South, Room 8040, Bethesda, MD 20892, USA
[6]Co-first author
*Correspondence: huangj3@mail.nih.gov
http://dx.doi.org/10.1016/j.stem.2015.04.002

SUMMARY

Maintaining genomic integrity is of paramount importance to embryonic stem cells (ESCs), as mutations are readily propagated to daughter cells. ESCs display hypersensitivity to DNA damage-induced apoptosis (DIA) to prevent such propagation, although the molecular mechanisms underlying this apoptotic response are unclear. Here, we report that the regulatory RNA *Apela* positively regulates p53-mediated DIA. *Apela* is highly expressed in mouse ESCs and is repressed by p53 activation, and *Apela* depletion compromises p53-dependent DIA. Although *Apela* contains a coding region, this coding ability is dispensable for *Apela*'s role in p53-mediated DIA. Instead, *Apela* functions as a regulatory RNA and interacts with hnRNPL, which prevents the mitochondrial localization and activation of p53. Together, these results describe a tri-element negative feedback loop composed of p53, *Apela*, and hnRNPL that regulates p53-mediated DIA, and they further demonstrate that regulatory RNAs add a layer of complexity to the apoptotic response of ESCs after DNA damage.

INTRODUCTION

Embryonic stem cells (ESCs) have a unique surveillance system for maintaining genome stability. Compared to differentiated cells, ESCs easily undergo apoptosis and differentiation upon DNA damage (Hong and Stambrook, 2004; Liu et al., 2013), which probably minimizes the risk of genome instability because it removes cells with damaged DNA from the population and enables a population with low DNA mutation burden (Cervantes et al., 2002). Indeed, the mutation frequency of the ESC population is about 100 times lower than that of differentiated cells (Cervantes et al., 2002). We and others have previously shown that p53 plays important roles in promoting the differentiation of mouse ESCs (mESCs) by repressing *Nanog* and other master regulators (Li et al., 2012; Lin et al., 2005). However, our understanding of the roles of p53 in DNA damage-induced apoptosis (DIA) of ESCs is incomplete, mainly because the mechanisms and the in vivo support are lacking. On the one hand, p53 is not required for the self-renewal of mESCs since mouse embryos with p53 knockout bypass the ESC stage (Donehower et al., 1992). On the other hand, p53 may have a pro-apoptotic function in mESCs based on a recent in vivo study showing that activated p53 is capable of regulating apoptotic genes in blastocysts (Goh et al., 2012). Given that mESCs have their unique transcriptional program and epigenome (Young, 2011), it is possible that the p53 signaling pathway regulates DNA damage-induced apoptosis (DIA) of ESCs by using part of the ESC-specific transcriptome. Therefore, identifying the ESC-specific part of the p53 transcriptional program will provide insights into how p53 regulates DIA of mESCs.

The observation that p53 activates *Puma*, a pro-apoptotic gene, in blastocysts leads us to investigate whether p53 regulates DIA of mESCs (Goh et al., 2012). After establishing that p53 is required for DIA of mESCs, we employ an integrative genome-wide approach to identify p53 targets that may mediate p53 function in DIA of mESCs. We focus on *Apela* (Apelin receptor early endogenous ligand) that encodes a putative peptide and find that *Apela* is involved in p53-mediated DIA of mESCs. Unexpectedly, the coding ability of *Apela* is dispensable for its pro-apoptotic function in mESCs. We further show that *Apela* acts as a regulatory RNA that modulates p53 activity by interacting with heterogeneous nuclear ribonucleoprotein L (hnRNPL), an inhibitory regulator of p53. Our results reveal a regulatory RNA-mediated negative feedback loop that regulates p53-mediated

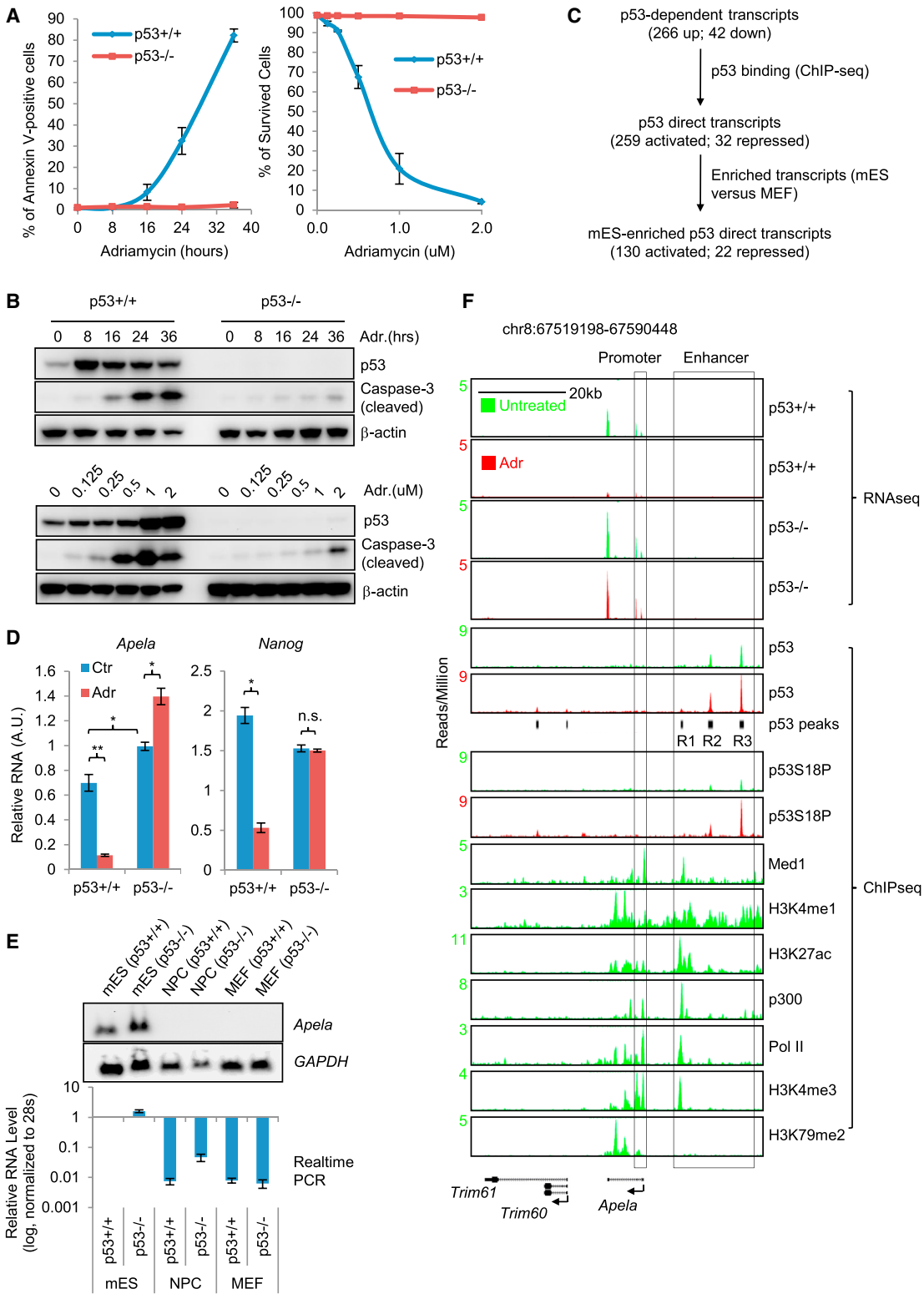

Figure 1. *Apela* Is Repressed by p53 and Enriched in mESCs

(A) Left, Annexin V staining to measure the percentage of apoptotic cells. Right, the percentage of survived cells treated with different concentrations of ADR for 24 hr. Error bars are SEM; n = 3.

(B) Western blot (W.B.) of mESCs treated with 0.5 μM ADR for various times (upper panels) and with various concentrations of ADR for 24 hr (lower panels).

(C) Identifying mESC-enriched p53 direct targets upon DNA damage.

(legend continued on next page)

DIA of mESCs, and they demonstrate that regulatory RNAs are part of p53 signaling in mESCs.

RESULTS

p53 Regulates DIA of mESCs

To test whether DIA of mESCs is p53 dependent, we first measured the kinetics of apoptosis in $p53^{+/+}$ and $p53^{-/-}$ mESCs in response to DNA damage using Annexin V staining (Figure 1A, left panel, and Figure S1A). We found that p53 plays a prominent role in regulating DIA of ESCs: around 80% of $p53^{+/+}$ mESCs became apoptotic 36 hr after receiving treatment with 0.5 μM Adriamycin (ADR) while less than 5% of $p53^{-/-}$ mESCs were apoptotic (Figure 1A, left panel, and Figure S1A). To rule out the dose-specific effect, we treated both $p53^{+/+}$ and $p53^{-/-}$ mESCs with different doses of ADR for 24 hr and observed p53-dependent DIA at all the tested doses (Figure 1A, right panel). However, the difference in the percentage of apoptotic cells between $p53^{+/+}$ and $p53^{-/-}$ mESCs is dependent on the dose of ADR (Figure 1A). Using cleaved caspase-3 as another apoptosis marker, we confirmed that p53 regulates DIA of mESCs, and apoptosis increased as early as 8 hr after DNA damage (Figure 1B). Our previous study showed that $p53^{+/+}$ and $p53^{-/-}$ mESCs have similar cell cycle profiles before and after ADR treatment (Li et al., 2012), excluding the contribution of cell cycle arrest to p53-mediated DIA of mESCs.

Apela Is Repressed by p53 and Is Highly Expressed in mESCs

We attempted to identify p53 downstream targets that may be involved in p53-mediated DIA of mESCs. For this, we used a genome-wide approach by integrating RNA-seq and ChIP-seq (Li et al., 2012) (Figure 1C). Using RNA-seq data from $p53^{+/+}$ and $p53^{-/-}$ mESCs that were either untreated or treated with ADR, we identified 266 upregulated and 42 downregulated p53-dependent transcripts in response to DNA damage (Figure 1C and Table S1). After integrating this with p53 ChIP-seq data, we cataloged 259 upregulated and 32 downregulated p53 direct targets (Figure 1C), which were defined as transcripts with expression change in a p53-dependent manner and associated with at least one p53 binding site (Table S1). Among the enriched pathways in these targets, regulation of cell death ($p = 0.0031$), apoptosis ($p = 0.0088$), and programmed cell death ($p = 0.0092$) pathways are relevant to the apoptotic function of p53 in mESCs (Table S1). Targets enriched in mESCs are more likely to modulate p53's mESC-specific function. Therefore, we excluded cell-type-nonspecific p53 targets by comparing the expression levels of all transcripts in mESCs to those in mouse embryonic fibroblasts (MEFs) (Figure 1C, also see Supplemental Experimental Procedures). This analysis resulted in 130 p53-activated and 22 p53-repressed transcripts that are enriched in mESCs (Table S1 and Table S2). We were interested in p53-repressed transcripts because p53-repressed transcripts are more likely to play ESC-specific functions than p53-activated transcripts and their regulation is relatively less well understood (Li et al., 2012; Zhang et al., 2013). Among the 22 p53-repressed, ESC-enriched transcripts, several transcripts, such as *Snora15*, *Dnmt3b*, *Prdm14*, *Lef1*, *Foxd3*, *Notch4*, *Cdk6*, and *Hmga1*, have been shown to play critical roles in the regulation of self-renewal and differentiation of ESCs (Table S2). We decided to focus on *Apela* (also called *Gm10664*), which had been annotated as a long non-coding RNA in the NCBI database. However, its zebrafish homolog has recently been shown to encode a secretory peptide called Toddler (Pauli et al., 2014) or ELABELA (Chng et al., 2013), which regulates cell movement during gastrulation. Hereinafter, we use the latest official name in NCBI, *Apela*, to refer to this RNA species. Because our previous study had shown that p53 has a non-cell-autonomous function in mESCs (Lee et al., 2010), our initial impression was that we had discovered a secretory signaling peptide, Apela, which is part of the cell-non-autonomous function of p53 in mESCs.

Using real-time PCR, we validated that *Apela* was repressed by DNA damage in a p53-dependent manner (Figure 1D and Figure S1B). In addition, in the absence of extrinsic stress, the amount of *Apela* was significantly higher in $p53^{-/-}$ mESCs than in $p53^{+/+}$ mESCs (Figure 1D, compare blue bars in the left panel), suggesting that p53 actively represses *Apela* even without extrinsic DNA damage. Both northern blot and real-time PCR verified that *Apela* was highly expressed in mESCs but not in neural progenitor cells (NPCs) and MEFs (Figure 1E). Specifically, the levels of *Apela* were about 100 times higher in mESCs than in NPCs or MEFs (Figure 1E). The expression levels of *Apela* were less than those of *Pou5f1* (also called *Oct4*) and *Nanog* mRNAs but were comparable to those of *Tfcp2l1* and *Klf4* mRNAs, which also encode ESC transcription factors (Figure S1C) (Chen et al., 2008). Northern blot analysis and shRNA-mediated knockdown demonstrated that *Apela* had only one splicing variant in mESCs and the size of *Apela* in mESCs was the same as that of in vitro transcribed *Apela* (Figures S1D and S1E).

p53 Binds to the Enhancer Region of the *Apela* Locus

Next, we inspected our mRNA-seq and public RNA-seq data and found that *Apela* is spliced in mESCs as annotated in NCBI (Figure 1F and Figure S1F). Using ChIP-seq datasets of RNA polymerase II (Pol II), mediator (Med1), and epigenetic marks, we depicted a precise transcriptional unit, including the enhancer domain, the promoter, and the gene body, for *Apela* gene (Figure 1F). H3K4me3 marks the promoter while H3K79me2 marks the gene body (Berger, 2007; Heintzman et al., 2007; Rahl et al., 2010). H3K4me1, H3K27ac, Med1, and p300 together indicated that the *Apela* gene has a distal enhancer domain in mESCs (Figure 1F) (Berger, 2007; Heintzman et al., 2007; Kagey et al., 2010). p53 did not bind to the

(D) Real-time PCR to measure the levels of *Apela* and *Nanog* (control). Ctr, untreated; Adr, treated with 0.5 μM ADR for 8 hr. A.U., arbitrary unit. Error bars are SEM; n = 3. t test; *$p < 0.05$; **$p < 0.01$.

(E) Upper, northern blot with total RNA; lower, real-time PCR. Error bars are SEM; n = 3.

(F) RNA-seq and ChIP-seq on the *Apela* locus. Black bars underneath the p53 (Adr) view are identified p53 peaks; R1-3, Region 1–3. Promoter and enhancer are annotated using histone modifications, Med1, and Pol II.

See also Figure S1, Table S1, and Table S2.

promoter of *Apela*. Instead, it had three binding regions (R1–3) within the enhancer domain of the *Apela* gene (Figure 1F), which is consistent with our previous finding that enhancer interference is one of the mechanisms of p53-mediated transcriptional repression in mESCs upon DNA damage (Li et al., 2012). The weak binding region (R1) overlapped with the strong signal of Med1, H3K4me1, H3K27ac, p300, Pol II, and H3K4me3 while the medium binding region (R2) overlapped with the weak signal of Med1, H3K4me1, H3K27ac, p300, and Pol II, suggesting a reverse correlation of the signals of p53 and the enhancer markers (also see Supplemental Information). This annotated enhancer domain was also bound by many master transcription factors of mESCs, such as Nanog, Sox2, Oct4, etc. (Figure S1G).

Apela Acts as a Regulatory RNA for p53-Mediated DIA of mESCs Independent of Its Coding Ability

Because *Apela* is ESC enriched, we first examined whether *Apela* affects the self-renewal of mESCs. Knockdown of *Apela* had no detectable effect on the self-renewal of mESCs based on immunofluorescence staining and immunoblotting of key transcription factors, mESC proliferation, and colony formation (Figure 2A, Figures S2A–S2D). Microarray analysis did not identify any master regulators of mESCs or lineage markers that were regulated by *Apela* knockdown (Table S3). However, during embryoid body (EB) formation, in which the three germ layers form, *Apela* knockdown reduced the mesoderm markers (*Flk1* and *alpha-actin*) and endoderm markers (*Foxa2* and *Gata4*), but not the ectoderm markers (Figure S2E). This result is consistent with the studies in zebrafish showing that *Apela* regulates mesoderm and endoderm development (Chng et al., 2013; Pauli et al., 2014). Therefore, *Apela* does not affect mESCs under undifferentiated conditions.

We then reasoned that *Apela* may be involved in a p53-mediated stress response of mESCs since *Apela* is repressed by p53. To test this, we examined the response of mESCs with *Apela* knockdown to DNA damage. Both Annexin V staining and immunoblotting of cleaved caspase-3 showed that the reduction of *Apela* decreased DIA of mESCs in a p53-dependent manner (Figures 2B, 2C, and 2D). Thus, *Apela* is involved in p53-mediated DIA of mESCs. We then tested whether *Apela* regulates the transcription of p53-regulated apoptotic genes. We did not observe any consistent effect of *Apela* knockdown on the expression of *Cdkn1a* (*p21*), *Mdm2*, *Bcc3* (*Puma*), *Btg2*, and *Bax* in both untreated and ADR-treated mESCs (Figure S3A). Recently, p53 has been shown to regulate DIA in ESCs through its non-transcriptional role in mitochondria (Han et al., 2008; Liu et al., 2013). We therefore tested whether *Apela* regulates the non-transcriptional function of p53. For this, we first isolated cytoplasmic and nuclear fractions from ESCs and found that *Apela* knockdown decreased the cytoplasmic fraction, but not the total amount, of p53 under DNA damage (Figure 2E). Further, we isolated the mitochondrial fraction and observed that *Apela* knockdown decreased the amount of p53 in the mitochondria of mESCs (Figure 2F), suggesting that *Apela* regulates p53-mediated apoptosis in mESCs by altering its mitochondrial localization.

After establishing the role of *Apela* in p53-dependent DIA of mESCs, we wanted to gain insights into the underlying mechanism. In zebrafish, Apela is a short, secretory peptide and acts as a mitogen through the G protein-coupled Apelin receptor (Aplnr) during gastrulation (Chng et al., 2013; Pauli et al., 2014). Thus, one possibility is that *Apela* regulates DIA of mESCs through the Apela/Aplnr axis, a mechanism similar to our previously discovered non-cell-autonomous axis of p53/Wnt/Wnt receptor in mESCs (Lee et al., 2010). For this, we planned to knock down *Aplnr* to examine whether *Aplnr* knockdown phenocopies *Apela* knockdown. Surprisingly, we found that *Aplnr* is not expressed in mESCs based on RNA-seq analysis in the absence or presence of DNA damage (Figure 3A). As a control, its neighboring gene, *Tnks1bp1*, is expressed (Figure 3A). ChIP-seq data showed that the *Aplnr* locus was blanketed with a repressive histone modification, H3K27me3, and essentially had no active marks, H3K4me3, and H3K79me2 (Figure 3A). RNA Pol II was absent from the locus, firmly demonstrating that *Aplnr* is silenced in mESCs. To investigate the expression pattern of *Aplnr* during early developmental events, we measured the levels of *Aplnr* mRNA during EB formation (Figure 3B). At the ESC stage (0 day EB), there was no expression of *Aplnr* mRNA (Figure 3B), confirming the result from RNA-seq (Figure 3A). Notably, the expression of *Aplnr* mRNA gradually increased during differentiation (Figure 3B). In contrast, the levels of *Apela* increased about 2-fold from day 0 to day 8 (Figure 3C). These results show that *Aplnr*, the gene encoding the receptor for Apela, is completely silenced in mESCs but is expressed upon the differentiation of mESCs, explaining the observation that *Apela* knockdown regulated the expression of mesoderm and endoderm markers during EB formation (Figure S2E). Therefore, in mESCs, *Apela* has an Aplnr-independent function.

There are two possible explanations for the Aplnr-independent role of *Apela*. One is that the Apela peptide has another unidentified receptor that mediates Apela's function in regulating DIA of mESCs. We carried out BLASTp (Basic Local Alignment Search Tool-protein) search and did not find any protein that has a similar amino acid sequence to that of Aplnr, therefore arguing against the existence of another receptor of Apela peptide with a similar amino acid sequence. The other possibility is that the *Apela* RNA acts as a regulatory RNA to regulate p53-mediated DIA in mESCs that is independent of its coding ability and receptor Aplnr. *Apela* has a putative coding region (235–399 nucleotides [nts]). Within this putative coding region, there are two start codons (Figure 3D). To test the second possibility, we disrupted the putative translation of *Apela* RNA by introducing different modifications to *Apela*: (1) changing the first start codon of *Apela* from ATG to GGG (Apela_noATG); (2) changing both start codons from ATG to GGG (Apela_2noATG); and (3) deleting the whole putative coding region of *Apela* (Apela_Δcoding) (Figure 3D). We then performed rescue experiments using these different versions of modified *Apela* to test whether *Apela* without the putative coding ability can rescue the decreased apoptosis caused by *Apela* knockdown (Figures 3E and 3F and Figure S3B). Importantly, both wild-type *Apela* (Apela_WT) and modified *Apela* rescued the phenotype of *Apela* knockdown (Figure 3F and Figure S3B), demonstrating that the coding ability of *Apela* is dispensable for its function in regulating DIA of mESCs. These results together demonstrate that *Apela* acts as a regulatory RNA to regulate p53-mediated DIA of mESCs even though it has a coding capacity.

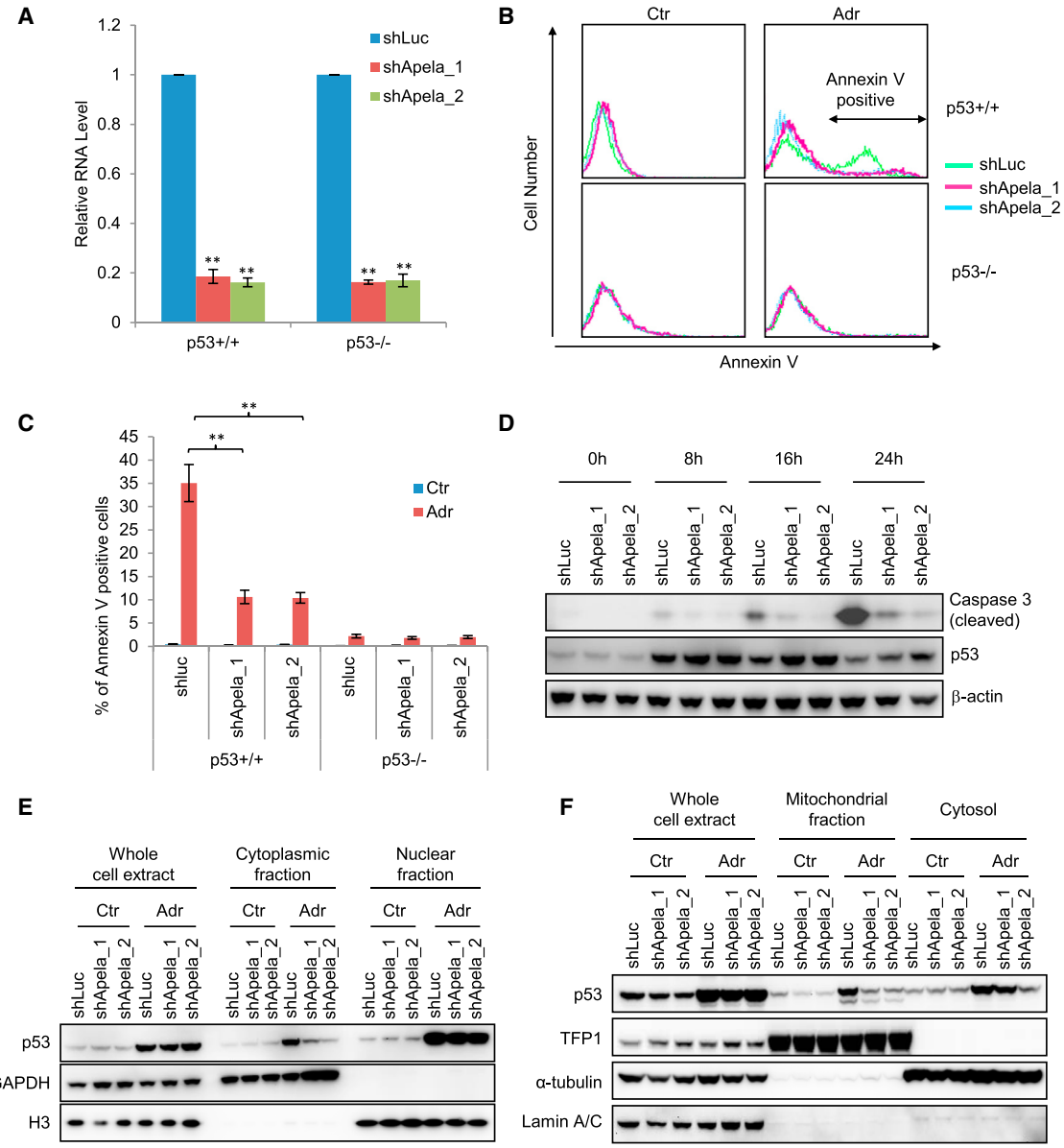

Figure 2. *Apela* Is Involved in p53-mediated DIA of mESCs

(A) Real-time PCR showing *Apela* knockdown. Error bars are SEM; n = 3. t test; *p < 0.05; **p < 0.01.

(B) Histograms of the Annexin V staining of mESCs in the presence (shApela_1 and shApela_2) or absence (shLuc) of *Apela* knockdown. Ctr, untreated; Adr, treated with 0.5 uM ADR for 24 hr.

(C) Quantification of (B). Error bars are SEM; n = 3. t test; *p < 0.05; **p < 0.01.

(D) W.B. of cleaved caspase-3, p53, and β-actin.

(E) W.B. showing the effect of *Apela* knockdown on the sub-cellular localization of p53. Each lane of cytoplasmic and nuclear fractions was loaded with proteins from same number of cells. GAPDH, a cytoplasmic marker; H3, a nuclear marker.

(F) W.B. showing the effect of *Apela* knockdown on the sub-cellular localization of p53. TFP1, a mitochondrial marker; α-tubulin, a cytosolic marker; Lamin A/C, a nuclear marker. Each lane of mitochondrial and cytosolic fractions contains the same amount of protein.

See also Figure S2 and Table S3.

To test whether Apela peptide, if produced, has a role in DIA of mESCs, we performed the rescue experiments using synthesized Apela peptide (Figure 3G). We did not observe any rescue effect of the Apela peptide at a wide range (1–1,000 ng/ml), suggesting that the mature Apela peptide, if produced, has no function in p53-mediated DIA of mESCs.

Apela Interacts with hnRNPL

Since some regulatory RNAs function through their binding partners (Huarte et al., 2010; Klattenhoff et al., 2013; Rinn et al., 2007), we chose to gain further insights into the role of *Apela* in p53-mediated DIA of ESCs by using an RNA pull-down assay (RPA) to identify the protein or proteins that bind to *Apela*.

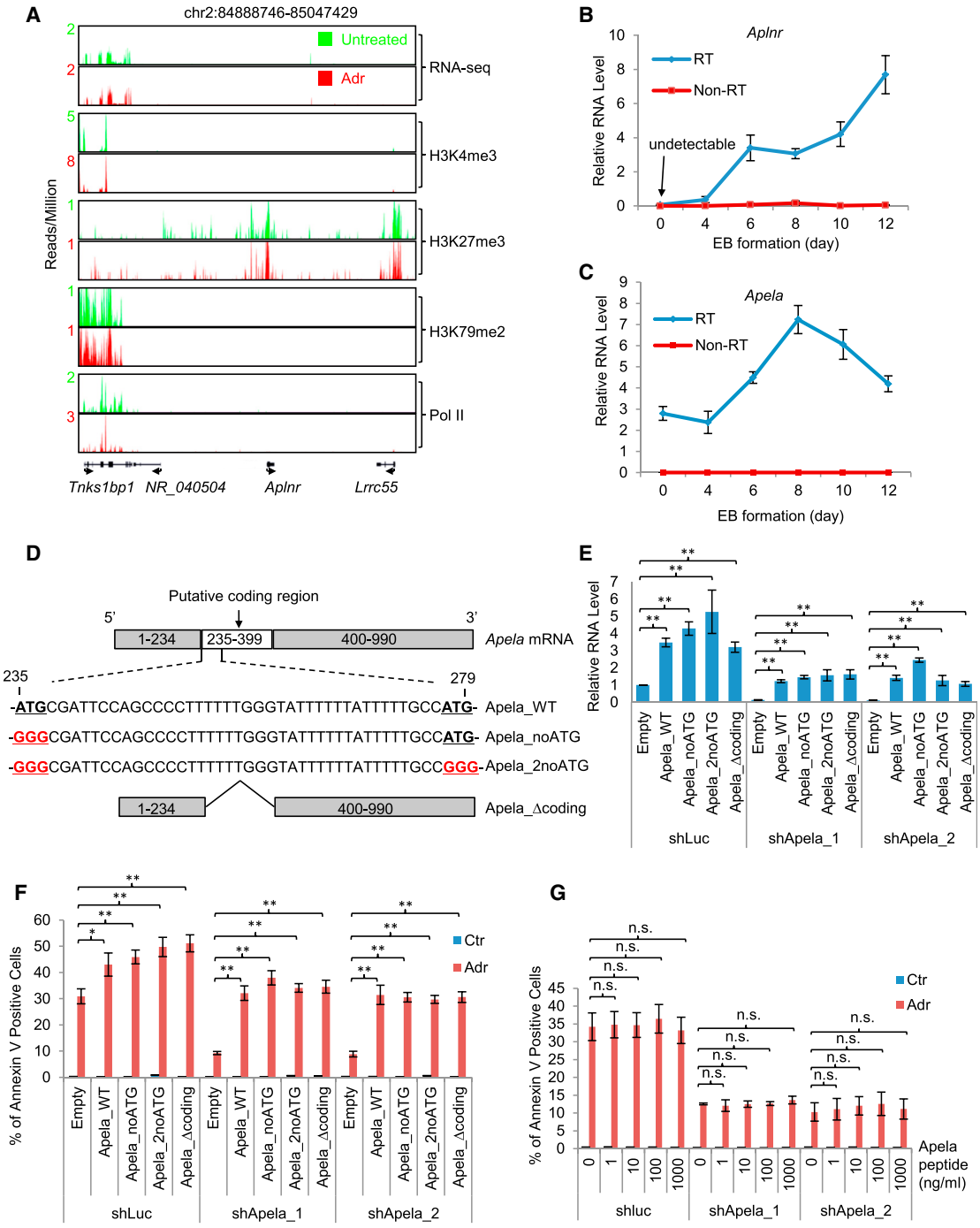

Figure 3. The Coding Ability of *Apela* Is Dispensable for Its Function in p53-Mediated DIA of mESCs

(A) RNA-seq and ChIP-seq of histone modifications and RNA Pol II on the *Aplnr* locus.

(B and C) Real-time PCR measuring the expression of *Aplnr* (B) and *Apela* (C) during EB formation. 0 day, the mESC stage; non-RT, no reverse transcriptase. Error bars are SEM; n = 3.

(D) Schematics showing modifications of the coding region of *Apela*: Apela_WT, wild-type *Apela*; Apela_nonATG, *Apela* with the first start codon ATG changed to GGG; Apela_2noATG, *Apela* with both start codons changed to GGG; Apela_Δcoding, *Apela* without the coding region.

(E) Real-time PCR measuring the relative RNA level of *Apela* in the rescue experiments: empty vector and vectors expressing modified *Apela* were stably transduced into mESCs containing shLuc, shApela_1, and shApela_2 using a PiggyBac system. Error bars are SEM; n = 3. t test; *p < 0.05; **p < 0.01.

(F) Rescue experiment: Annexin V staining of mESCs (shLuc, shApela_1, and shApela_2) transduced with the empty vector or a vector expressing an *Apela* variant (Apela_noATG, Apela_2noATG, or Apela_Δcoding). Error bars are SEM; n = 3. t test; *p < 0.05; **p < 0.01.

(G) Effect of Apela peptide (1–1,000 ng/ml) on DIA of mESCs. Error bars are SEM; n = 3. t test; *p < 0.05; **p < 0.01; n.s., not significant.

See also Figure S3.

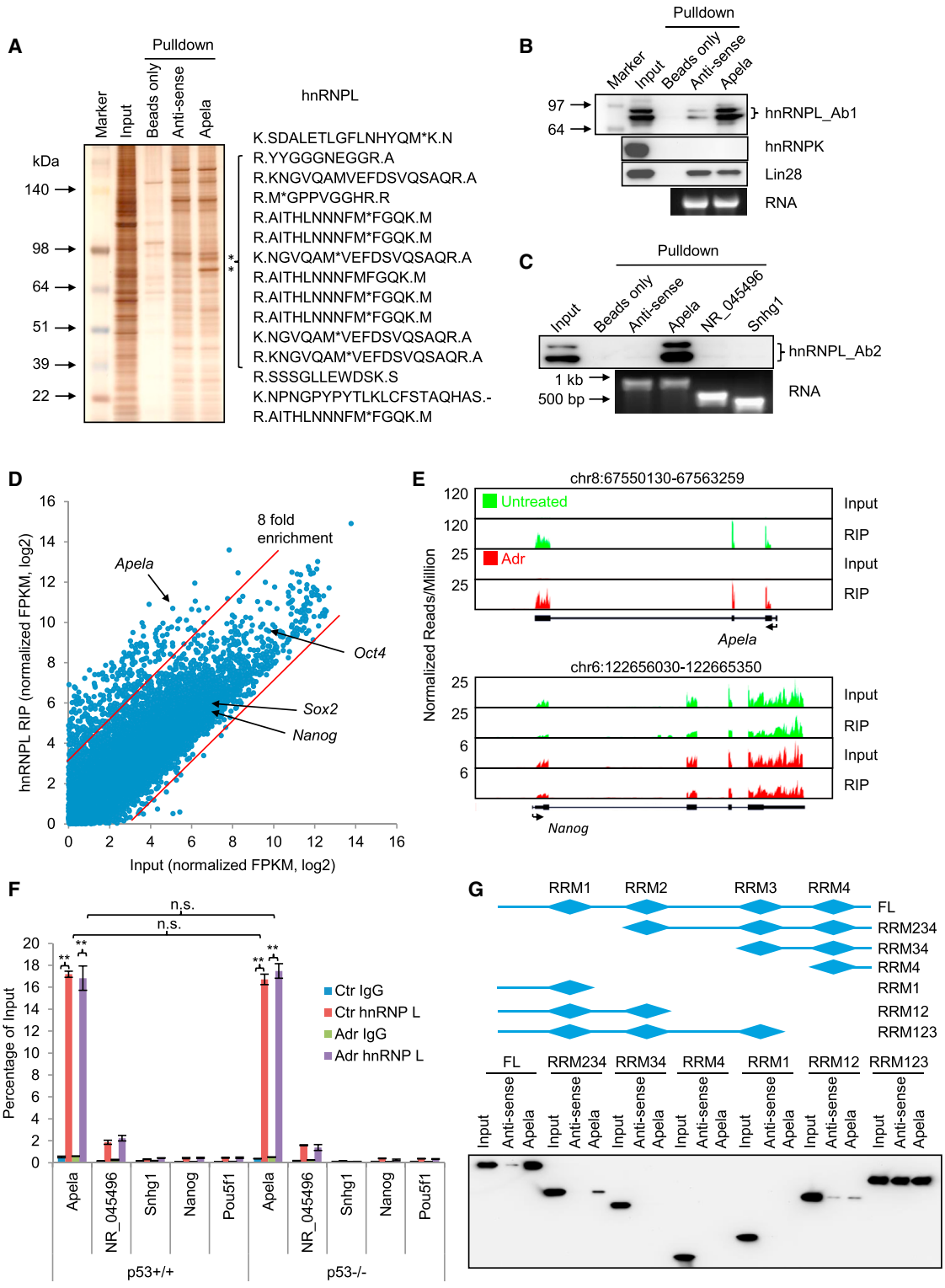

Figure 4. *Apela* Binds to hnRNPL Independent of p53 Status and DNA Damage

(A) Silver staining of RPA. Right, representative peptides identified by mass spectrometry.

(B) W.B. showing RPA from (A) with hnRNPL antibody (Ab), hnRNPK Ab (control), and Lin28 Ab (control). Ab1, first Ab for hnRNPL.

(C) W.B. showing RPA using *Apela* and two other RNA controls, *NR_045496* and *Snhg1*. Ab2, another Ab for hnRNPL.

(D) RIP-seq showing average-normalized, log2-transformed FPKM of hnRNPL-RIP and Input. The two red lines are the arbitrary cutoffs of 8-fold enrichment.

(legend continued on next page)

We first used a candidate approach to examine whether *Apela* binds to several ESC master regulators, such as Oct4, Nanog, Sox2, Klf4, and Utf1 (Figure S4A), and chromatin binding proteins, such as Suz12, Gcnf, G9a, and Dnmt3b (Figure S4B). We neither observed any enrichment of these proteins in *Apela* RPA as compared to anti-sense *Apela* RPA (control) (Figures S4A and S4B) nor found any evidence that *Apela* binds to the p53 protein (Figure S4B). Thus, this candidate approach did not identify any protein that binds *Apela*. Next, we employed an unbiased approach, which combines RPA with silver staining followed by mass spectrometry (Figure 4A) (Rinn et al., 2007; Tsai et al., 2010). This approach revealed that *Apela* pulled down two bands, which represented the same protein, hnRNPL (Figures 4A and S4C). Both hnRNPL splicing variants were enriched to a similar degree (Figures 4B and 4C).

We confirmed the interaction between *Apela* and hnRNPL using RPA followed by immunoblotting with two different antibodies (Ab1 and Ab2) recognizing hnRNPL (Figures 4B and 4C). Two lines of evidence suggest that the interaction between *Apela* and hnRNPL is specific. First, two other RNA binding proteins, hnRNPK and Lin28, did not show enrichment in *Apela* pull-down (Figure 4B). Second, two other RNAs, *NR_045496* and *Snhg1*, did not bind to hnRNPL (Figure 4C).

To verify the interaction reciprocally, we carried out RNA immunoprecipitation (RIP) and sequencing (RIP-seq) in $p53^{+/+}$ mESCs (Figures 4D and 4E). 405 transcripts were identified as hnRNPL-bound when using an 8-fold increase as a cutoff (Figure 4E and Table S4). *Apela* was enriched about 48 times in the immunoprecipitated complex while controls, such as *Nanog*, *Sox2*, and *Oct4* mRNA, were not enriched (Figures 4D and 4E). RIP-seq results were confirmed by RIP followed by real-time PCR (Figure 4F). hnRNPL Ab enriched *Apela* around 100-fold compared to enrichment levels of IgG control (Figure 4F). Moreover, the relative enrichment (percentage of input) was not affected by DNA damage (Figure S4C and Figure 4F, compare Ctr to Adr) and was independent of the p53 status (Figure S4C and Figure 4F, compare $p53^{+/+}$ to $p53^{-/-}$). In contrast, the interaction between hnRNPL and a control RNA, *NR_045496*, was weak. The interaction between hnRNPL and *Snhg1*, *Nanog*, or *Oct4* mRNAs was similar to background (IgG). Using recombinant hnRNPL and in vitro transcribed *Apela*, we detected a direct interaction between hnRNPL and *Apela* (Figure S4D). In summary, hnRNPL is a bona fide binding partner of *Apela*.

hnRNPL contains four RNA recognition motifs (RRM1–4) (Figure 4G, upper panel). To map the region or regions within hnRNPL that contribute to *Apela* binding, we tested the binding of *Apela* and anti-sense *Apela* (as a negative control) to a variety of hnRNPL truncation variants. The first three RRMs of hnRNPL were required for *Apela* binding (Figure 4G). Interestingly, the fourth RRM was not required for *Apela* binding. Instead, it determined the binding specificity since RRM1/2/3 of hnRNPL bound to anti-sense *Apela* as well.

To further test whether *Apela* and p53 interact, we performed p53 RIP assay (Figure S4E). p53 IP did not pull down *Apela*, consistent with the result of RPA (Figure S4B). Because alternative RNA splicing is one of the major functions of hnRNPL (Motta-Mena et al., 2010), we investigated the effect of hnRNPL knockdown on *Apela* splicing and sub-cellular localization. hnRNPL did not affect *Apela* splicing but slightly altered the sub-cellular localization of *Apela* (Figures S4F–S4J).

The 3′ UTR of *Apela* Interacts with hnRNPL and Is Required for *Apela*'s Role in p53-mediated DIA of mESCs

To map the region or regions within *Apela* that interact with hnRNPL, we performed RPA using different fragments of *Apela* (Figure 5A). A region (732–974 nt) within the 3′ UTR (400–974 nt) of *Apela* bound to hnRNPL as efficiently as the full length of *Apela* (Figure 5A). Further mapping of this region (732–974 nt) indicated that a domain within 793–859 nt was required for the interaction (Figure 5B). Since the region binding to hnRNPL falls into the 3′ UTR, we then asked whether the 3′ UTR of *Apela* has a function similar to that of the wild-type in DIA of mESCs. For this, we performed RPA (Figure 5C) and the rescue experiment (Figures 5D and 5E) using the 3′ UTR and the full length of *Apela*. The 3′ UTR of *Apela* bound to hnRNPL and rescued the reduction of DIA as efficiently as wild-type *Apela* (Apela_WT) (Figures 5D and 5E), further corroborating the conclusion that the coding ability of *Apela* is dispensable for its function in DIA of mESCs (Figure 3). RPA showed that the 3′ UTR of *Apela* does not interact with the ribosomal proteins Rpl26 and Rps3 (Figures S5A and S5B), ruling out the possibility that *Apela* regulates DIA of mESCs by interfering with translation in general.

The Interaction between *Apela* and hnRNPL Is Required for *Apela*'s Role in p53-mediated DIA

Because hnRNPL has been shown to bind to the CA tracts in the intronic regions of other genes (Hui et al., 2005), we searched the 732–974 nt domain and found that two CA tracts are around this domain (Figure S5C). RNA secondary structure prediction revealed that these two CA tracts were brought to proximity by a loop (Figure S5C). These results suggest that these two CA tracts are the sites interacting with hnRNPL. To test this, we generated *Apela* mutants containing GU substitutions at the first (Apela_M1), second (Apela_M2), or both CA (Apela_M12) tracts and performed RPA (Figures 5F and 5G). We found that both CA tracts were involved in the interaction with hnRNPL, and the second CA tract was dominant (Figure 5G). Substitution of both CA tracts with GU tracts completely disrupted the binding between hnRNPL and *Apela* (Figure 5G, compare Apela_M12 to anti-sense). Therefore, hnRNPL binds to *Apela* only at these two CA tracts.

To investigate the functional relevance of the interaction between *Apela* and hnRNPL to p53-mediated apoptosis in

(E) RIP-seq showing the enrichment of *Apela* in RIP with hnRNPL Ab. *Nanog* mRNA, a negative control; green, untreated; red, 0.5 μM ADR for 8 hr. Input and hnRNPL-RIP were scaled to the same level.

(F) RIP with hnRNPL Ab followed by real-time PCR. Percentage of input was calculated to measure the relative interaction between hnRNPL and RNAs. Error bars are SEM; n = 3. t test; *p < 0.05; **p < 0.01; n.s., not significant.

(G) Upper, schematics of hnRNPL variants; lower, RPA using *Apela* (anti-sense and sense) and Flag-tagged hnRNPL fragments.

See also Figure S4 and Table S4.

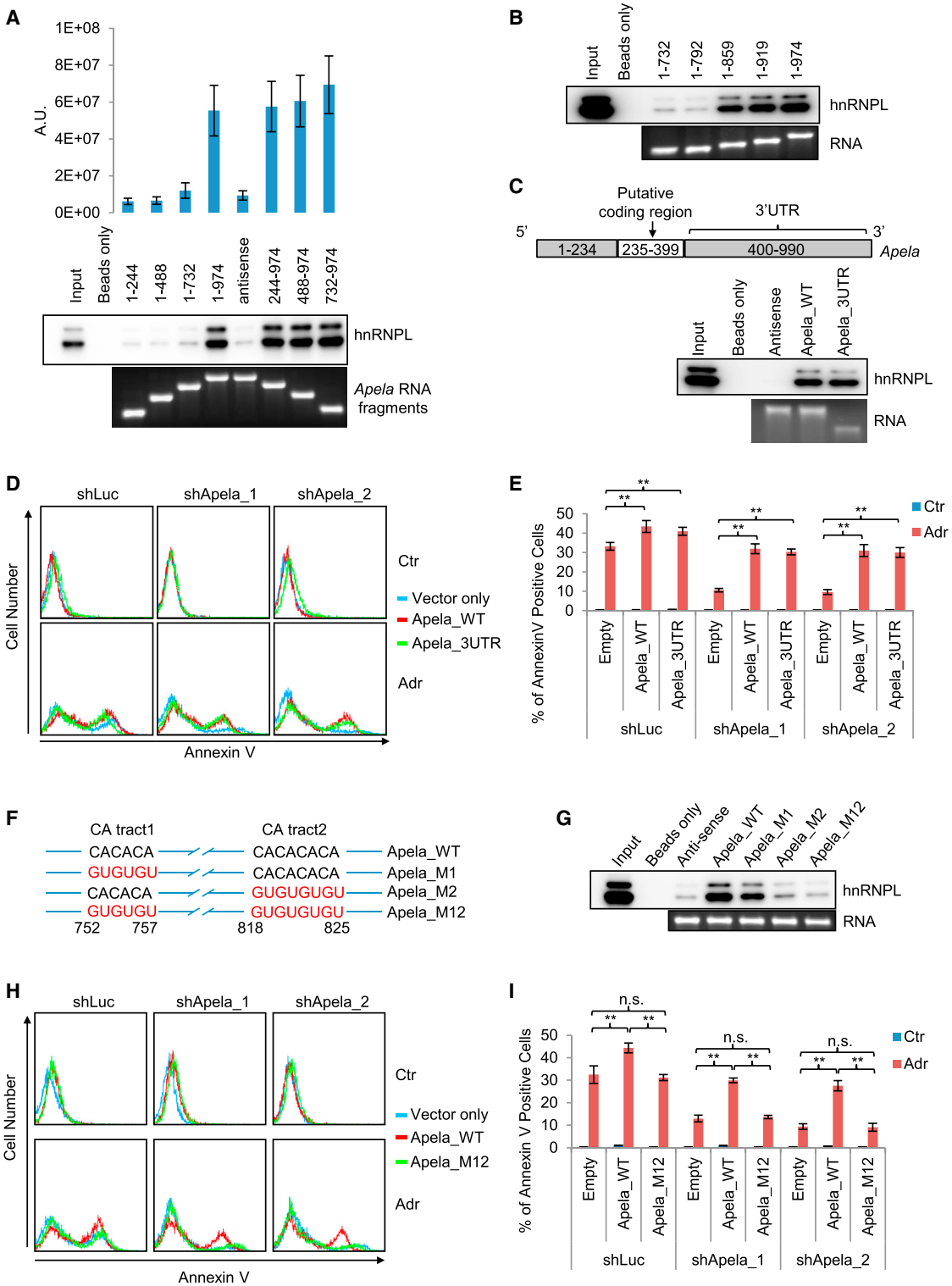

Figure 5. hnRNPL Binds to the CA Tracts within the 3′ UTR of *Apela*

(A) RPA using different fragments of *Apela* to map the interacting domain in *Apela* with hnRNPL. Numbers are the nucleotide positions from 5′ and 3′ end. Error bars are SEM; n = 3.

(B) Mapping the region within *Apela* that binds hnRNPL.

(C) RPA using wild-type *Apela* (Apela_WT) and the 3′ UTR of *Apela* (Apela_3UTR).

(legend continued on next page)

mESCs, we performed rescue experiments using wild-type *Apela* (Apela_WT) and the *Apela* mutant containing two CA-to-GU substitutions (Apela_M12), which disrupted the interaction between *Apela* and hnRNPL. Apela_M12 did not rescue the decreased apoptosis caused by *Apela* knockdown (Figures 5H and 5I and Figure S5D), demonstrating that the binding between hnRNPL and *Apela* is required for the function of *Apela* in DIA of mESCs.

hnRNPL Inhibits p53 Activation and Mitochondrial Localization in mESCs

To investigate whether hnRNPL is involved in p53-mediated DIA of mESCs, we used shRNAs to reduce the levels of hnRNPL in both $p53^{+/+}$ and $p53^{-/-}$ mESCs (Figure 6A). hnRNPL knockdown activated p53 in the absence or presence of ADR treatment (Figure 6B), indicating that hnRNPL inhibits p53 activation. hnRNPL knockdown did not increase DNA damage in mESCs as judged by H2AX-S139P (Figure 6B), suggesting that the increased p53 is not caused by DNA damage. The activation of p53 coincided with the increase of p53K379ac, but not p53S18P (Figure 6C). Since acetylation blocks the degradation of p53 (Kruse and Gu, 2009), we tested whether hnRNPL knockdown affects the degradation of p53. Cycloheximide (CHX) was used to inhibit the translation of p53 in untreated control and hnRNPL knockdown mESCs and p53 half-life was measured (Figure 6D). We found that hnRNPL knockdown prolonged the half-life of p53 from about 18 to 33–40 min, demonstrating that hnRNPL knockdown inhibits the degradation of p53 in mESCs. We were unable to precisely quantify the effect of hnRNPL knockdown on p53 half-life in ADR-treated mESCs due to rapid cell death induced by the combinatory treatment of ADR and CHX (Figure S6A). We found that hnRNPL knockdown increased the mitochondrial localization (Figure 6E) in addition to the stability of p53 (Figure 6B). Therefore, hnRNPL has a wider role than *Apela* in regulating p53 in mESCs: hnRNPL regulates both stability and mitochondrial localization of p53 while *Apela* only affects mitochondrial localization.

To examine the functional consequence of the increased p53 levels in response to hnRNPL knockdown, we performed Annexin V staining and found that hnRNPL knockdown significantly increased apoptosis in $p53^{+/+}$, but not $p53^{-/-}$, mESCs (Figures 6F and 6G). Thus, hnRNPL prevents mESCs from apoptosis by inhibiting p53 activation. Since both *Apela* and hnRNPL are involved in p53-mediated apoptosis in mESCs and since they bind to each other, we aimed to dissect the hierarchy of these two binding partners in p53-mediated apoptosis. To achieve this, we performed the Annexin V staining of mESCs with the combinatory knockdown of *Apela* and hnRNPL. We reasoned that if hnRNPL is upstream of *Apela*, the combinatory knockdown of *Apela* and hnRNPL would produce results similar to those of *Apela* knockdown; if *Apela* is upstream of hnRNPL, the combinatory knockdown will have an outcome similar to that of hnRNPL knockdown. Our results supported the latter possibility that *Apela* affects p53-mediated DIA in mESCs upstream of hnRNPL (Figures S6B and S6C).

Apela Negatively Regulates the Interaction between hnRNPL and p53

Previous studies showed that hnRNPK, another member in the hnRNP family, binds to p53 (Moumen et al., 2005). Thus, we hypothesized that hnRNPL binds to p53. To test this hypothesis, we performed double immunostaining followed by confocal analysis and observed a strong co-localization between p53 and hnRNPL in mESCs in the absence or in the presence of ADR treatment (Figure 7A and Figures S7A and S7B). The co-localization of hnRNPL and p53 suggests that they bind to each other in mESCs. To test this, we carried out co-immunoprecipitation (co-IP) in mESCs using p53 Ab followed by immunoblotting with hnRNPL Ab and detected an interaction between p53 and hnRNPL (Figure 7B). DNA damage did not obviously alter hnRNPL protein levels but increased p53 protein levels in mESCs (Figure 7B). Despite the fact that more p53 existed in mESCs after DNA damage, the absolute amount of hnRNPL in the p53 immuno-complex did not change, suggesting that the relative portion of p53 interacting with hnRNPL decreases after DNA damage. We also performed co-IP with recombinant hnRNPL and recombinant p53 and observed a direct interaction between hnRNPL and p53 (Figure 7C). To identify the region or regions within p53 that are responsible for the interaction with hnRNPL, we generated recombinant p53 containing the amino terminal domain (ATD), DNA binding domain (DBD), or carboxyl terminal domain (CTD) and performed pulldown followed by hnRNPL immunoblotting (Figure 7D). We found that hnRNPL binds to the CTD of p53 (Figure 7D). In vitro pulldown assay using Flag-tagged hnRNPL mutants containing various RRMs and GST-tagged full-length p53 demonstrated that the first two RRMs of hnRNPL contribute to the binding with p53 (Figure 7E). In summary, the CTD of p53 interacts with the first two RRMs within hnRNPL (Figure 7F).

To explore how *Apela* affects the regulation of p53 by hnRNPL, we performed co-IP experiments in mESCs untreated or treated with ADR in the absence (shLuc) or in the presence (shApela_1 and shApela_2) of *Apela* knockdown (Figure 7G). We found that *Apela* knockdown increased the interaction between hnRNPL and p53 after ADR treatment (Figure 7G), indicating that *Apela* negatively regulates the interaction between hnRNPL and p53. This result is consistent with the observation that *Apela* and hnRNPL have opposite roles in regulating p53-mediated DIA of mESCs.

(D) Representative histograms of Annexin V staining of mESCs in the rescue experiment using vector only, Apela_WT, and Apela_3UTR in the absence (Ctr) or presence (Adr, 24 hr) of ADR treatment.
(E) Quantification of (D). Error bars are SEM; n = 3. t test; *p < 0.05; **p < 0.01.
(F) Sequences of wild-type (WT) *Apela* and mutants (M1, first CA tract disrupted; M2, second CA tract disrupted; M12, both CA tracts disrupted).
(G) RPA using WT and mutant *Apela*.
(H) Representative histograms of Annexin V staining of mESCs in the rescue experiment in the absence (Ctr) or presence of (Adr, 24 hr) ADR treatment.
(I) Quantification of (H). Error bars are SEM; n ≥ 3. t test; *p < 0.05; **p < 0.01; n.s., not significant.
See also Figure S5.

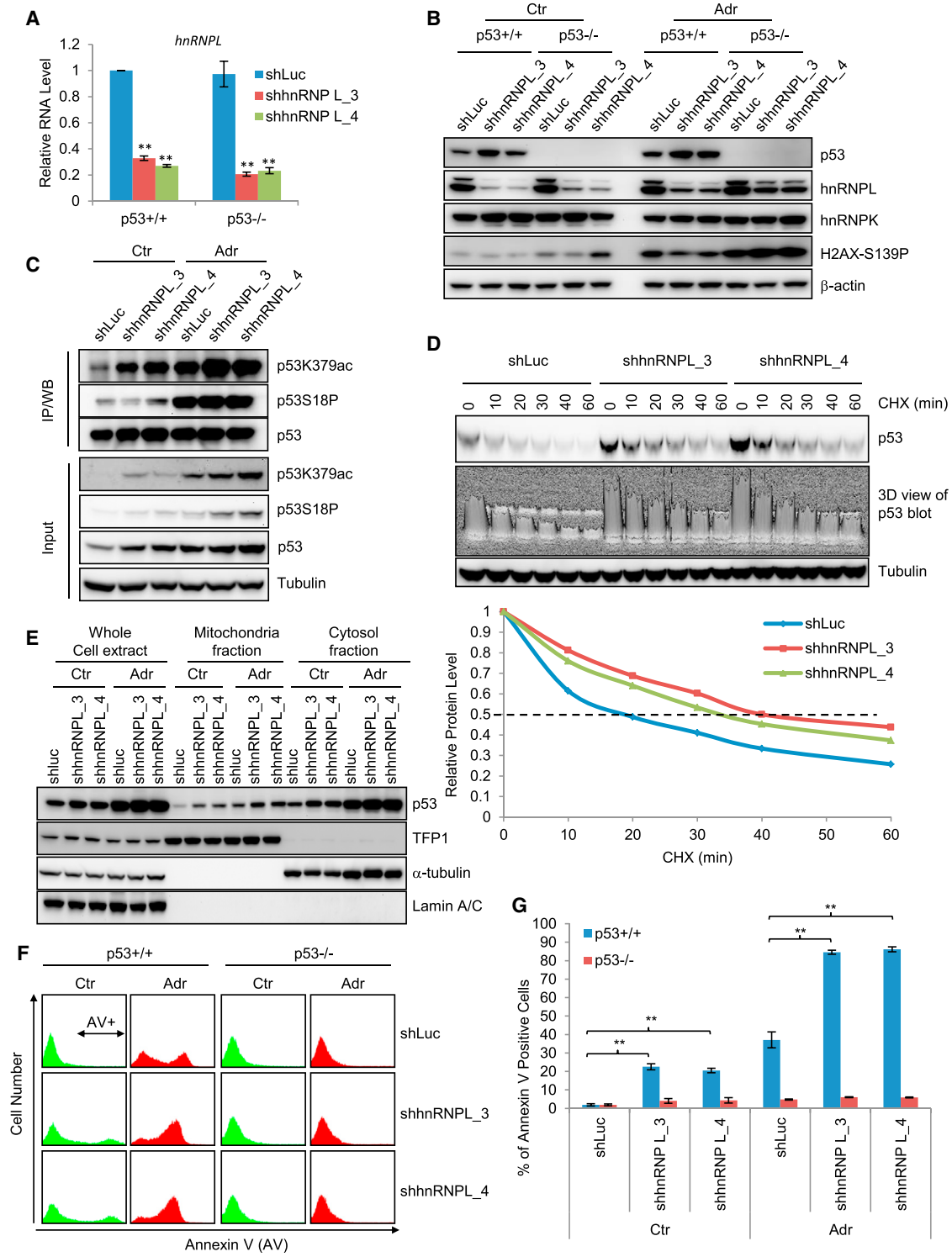

Figure 6. hnRNPL Inhibits p53 Activation and p53-Dependent Apoptosis of mESCs

(A) Real-time PCR measuring hnRNPL mRNA levels. Error bars are SEM; n = 3. t test; *p < 0.05; **p < 0.01.

(B) W.B. showing the effect of hnRNPL knockdown on p53.

(C) Immunoprecipitation (IP) followed by W.B. showing the effect of hnRNPL knockdown on p53 K379ac and S18P. Total p53 amount in each lane was adjusted to the same level for comparing K379ac and S18P levels.

(D) W.B. showing the effect of hnRNPL knockdown on p53 degradation; 3D view showing the band intensity of p53; lower panel, quantification of p53 levels.

(E) W.B. showing the effect of hnRNPL knockdown on the mitochondrial localization of p53.

(legend continued on next page)

DISCUSSION

A Tri-Element Negative Feedback Loop that Regulates p53-mediated DIA in mESCs

The mechanisms underlying DIA of mESCs are not fully appreciated, and the apoptotic role of p53 in mESCs has been still elusive, which can partially be attributed to the lack of understanding of the mechanisms. The discovery of a tri-element negative feedback loop involving p53, *Apela*, and hnRNPL contributes to the understanding of DIA of mESCs (Figure 7H). This tri-element negative feedback loop differs from the well-established di-element p53/Mdm2 loop in that it is mediated by a regulatory RNA, *Apela*. In addition, this tri-element loop appears to be cell type specific, consistent with the concept that the regulation of p53 signaling in mESCs is influenced by an ESC-specific transcriptome.

In mESCs, p53 activity needs to be kept in check because unwanted activation of p53 will cause the differentiation and/or apoptosis of mESCs. Nucleolin and aurora kinase A (Aurka) inhibit the pro-differentiation activity of p53 in mESCs (Cinghu et al., 2014; Lee et al., 2012; Montes de Oca Luna et al., 1995). However, it is unknown which factor or factors suppress the pro-apoptotic function of p53 in mESCs. The fact that Mdm2 and Mdm4 knockout embryos survive beyond the blastocyst stage suggests that other factors prevent p53 activation in mESCs (Jones et al., 1995; Montes de Oca Luna et al., 1995; Parant et al., 2001). Here we find that hnRNPL is a factor that antagonizes p53-mediated apoptosis in mESCs (Figures 6 and 7). Thus, multiple proteins are probably needed to subdue p53 activation in mESCs to ensure normal development under unstressed conditions. It is worth noting that hnRNPs are multifunctional proteins (Chaudhury et al., 2010; Ray et al., 2009). Therefore, the inhibition of p53 activation may only be one of the functions of hnRNPL. In the same vein, not every transcript bound by hnRNPL regulates p53 in mESCs (Figure S7C).

Apela binds to hnRNPL and antagonizes its inhibitory effect on p53 during DNA damage response (DDR). However, the precise mechanism of this antagonism is currently unknown. It is possible that *Apela* antagonizes the activity of hnRNPL by modulating its conformation or post-translational modifications or competing with hnRNPL-p53 dimers. Under unstressed conditions, the copy numbers of *Apela* and mitochondrial p53 in a single mESCs are about 110 and 40, respectively. After DNA damage, the copy numbers of *Apela* and mitochondrial p53 are about 25 and 160, respectively (Figures S7D–S7F and Supplemental Information). These results suggest that the copy number of *Apela* is enough to influence the mitochondrial localization of p53, although as an activator, *Apela* does not need to release all the p53 molecules to affect apoptosis. In addition, *Apela* may regulate many copies of hnRNPL by a dynamic interaction.

Since *Apela* positively regulates p53, the repression of *Apela* by p53 probably serves as a means to avoid uncontrolled "firing" of p53. Therefore, our results suggest that mESCs employ this p53/*Apela*/hnRNPL negative feedback loop to balance the needs of suppressing p53 in mESCs without extrinsic DNA damage stress and achieving rapid apoptosis upon DNA damage. We note that *Apela* is a modulator, not a determinant, of p53-mediated DIA of mESCs, and other mechanisms have been reported. For example, others have shown that the lack of G1/S arrest in mESCs, mitochondrial priming in human ESCs (hESCs), and the Golgi localization of Bax also contribute to the sensitivity of ESCs to DIA (Dumitru et al., 2012; Hong and Stambrook, 2004; Liu et al., 2013). It is possible that other unidentified mechanisms exist. Thus, further elucidation of these mechanisms will help us fully understand the DNA damage stress response of ESCs.

The Function of *Apela* in p53-mediated DIA Does Not Require Its Coding Ability

A striking finding in this study is that the coding ability is dispensable for the regulatory function of *Apela* in p53-mediated DIA of mESCs. Four lines of evidence support this conclusion. First, the *Aplnr* gene that encodes the cognate receptor for the Apela peptide is not expressed in mESCs (Figures 3A and 3B). Second, *Apela* without the putative coding region rescues the phenotype of *Apela* knockdown (Figures 3D–3F and Figures 5D and 5E), while the Apela peptide does not (Figure 3G). Third, the region within *Apela* that binds hnRNPL is at the 3′ UTR (Figure 5). Fourth, Apela peptide has no effect in DIA of ESCs. It is possible that *Apela* has multiple modes of action depending on the developmental stages: in mESCs, it regulates p53-mediated apoptosis independent of its coding ability, while during early development, it controls cell movement through encoded Apela peptide and the Apela/Aplnr axis. Indeed, *Apela* and *Aplnr* mRNAs are dynamically expressed during early development using the EB formation model (Figures 3B and 3C). Both Apela and Apelin are ligands for Aplnr in zebrafish; *Apela* is expressed in the early development of zebrafish while *Apelin* is expressed in the late development (Chng et al., 2013; Pauli et al., 2014).

Although we detected no activity of Apela peptide in p53-mediated DIA of mESCs, it is worth noting that our results do not exclude the possibility that in mESCs *Apela* is translated into the Apela peptide, nor do they contradict recent studies showing that in zebrafish *Apela* encodes a secretory peptide (Chng et al., 2013; Pauli et al., 2014). Instead, we identify another mode of action of *Apela*: it functions as a regulatory RNA in the context of p53-mediated DIA of mESCs. A ribosomal profiling in mESCs suggests that *Apela* is translated in mESCs (Ingolia et al., 2011). However, we did not successfully detect the putative endogenous Apela peptide in mESCs using mass spectrometry. In zebrafish, *Apela* (also called *Toddler* or *ELABELA*) is expressed only at the gastrulation stage whereas *Aplnr* is ubiquitously expressed (Chng et al., 2013; Pauli et al., 2014). In mESCs (this study) and hESCs (Chng et al., 2013), *Apela* is highly expressed while the receptor gene, *Aplnr*, is silenced in mESCs. We speculate that this noncoding mechanism of *Apela* facilitates

(F) Representative histograms of Annexin V staining of mESCs without (shLuc) and with hnRNPL knockdown in the absence (Ctr) or presence (Adr, 24 hr) of ADR treatment.

(G) Quantification of (F). Error bars are SEM; n = 3. t test; *p < 0.05; **p < 0.01; n.s., not significant.

See also Figure S6.

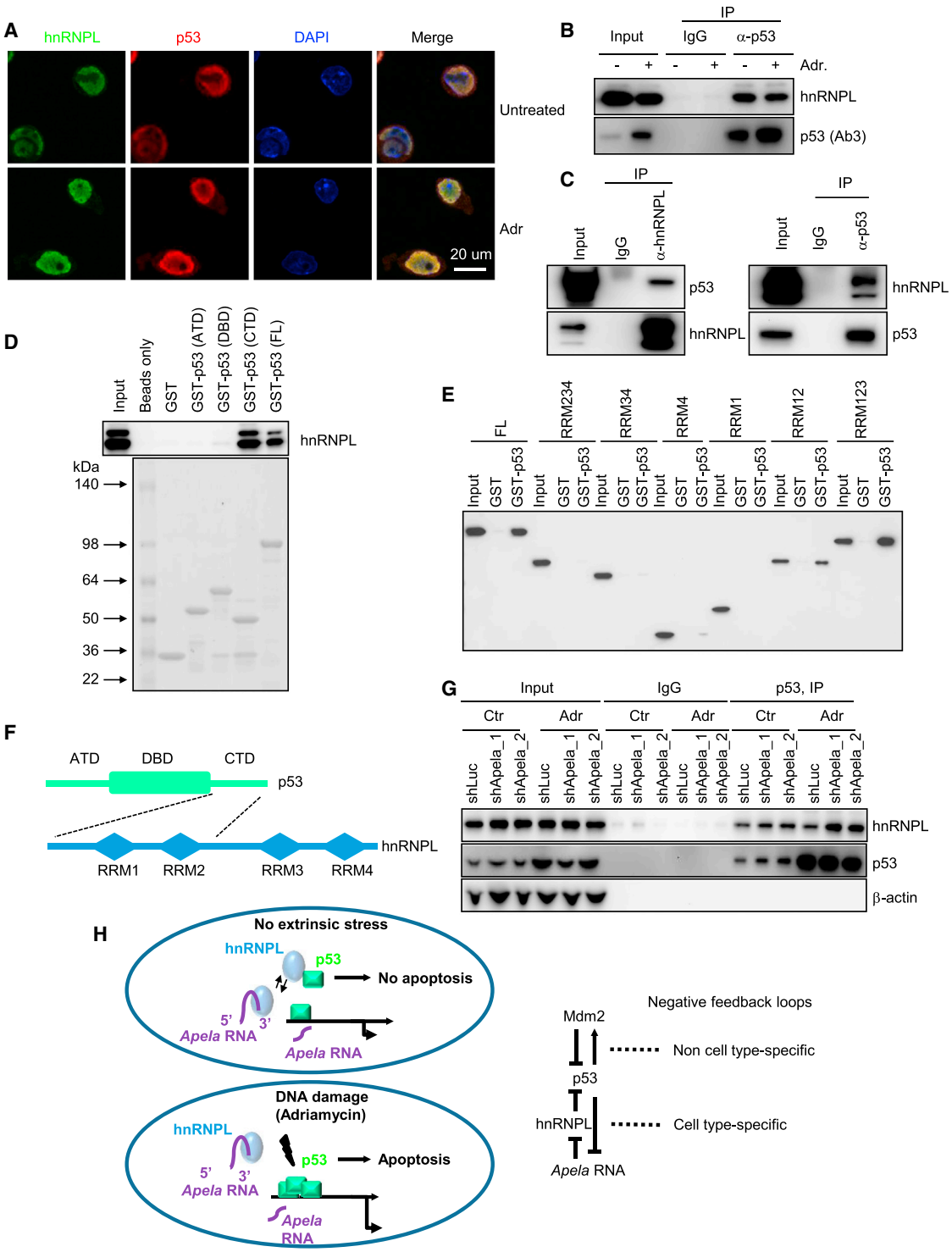

Figure 7. *Apela* Inhibits hnRNPL/p53 Interaction

(A) Immunostaining showing the co-localization of hnRNPL and p53 in mESCs untreated or treated with 0.5 μM ADR for 8 hr.

(B) Co-IP using p53 Ab followed by W.B. with hnRNPL Ab.

(C) Co-IP using recombinant hnRNPL and recombinant p53.

(D) Pulldown using purified GST-tagged p53 fragments and mESC lysate.

(E) Co-IP using purified GST-tagged FL p53 and Flag-tagged hnRNPL fragments followed by W.B. with Flag Ab.

(F) Domain structures of p53 and hnRNPL. The dashed black lines indicate the interacting domains within p53 and hnRNPL.

(legend continued on next page)

a fast DDR of ESCs because it bypasses the step of protein translation. It remains unclear whether this mode of action of *Apela* in mESCs is conserved across all mammals.

In the last several years, many studies have investigated how regulatory RNAs, especially noncoding RNAs, affect various cellular processes, such as apoptosis (Hung et al., 2011) and differentiation (Klattenhoff et al., 2013). In this study, we serendipitously discovered that an RNA species with a coding ability, *Apela*, has a noncoding function in mESCs, raising the possibility that other coding RNAs may also have functions beyond their coding ability. Therefore, our results could potentially expand the concept of regulatory RNAs and fuel another line of investigation.

EXPERIMENTAL PROCEDURES

ChIP-Seq, RNA-Seq, and Data Analyses

ChIP-seq and data analyses were performed as previously described (Li et al., 2012). Deep sequencing was done in the Next Generation Sequencing Facility (NGSF) at the Center for Cancer Research (CCR) in NCI. Briefly, 10 ng of IP genomic DNA was used in library construction and cluster generation and was sequenced in the Genome Analyzer IIx (GAIIx) or HiSeq 2000 system. For RNA-seq, 1 μg of total RNA was sent to the NGSF. All the procedures were carried out according to Illumina's protocols. Data analyses and Z-score algorithm are described in the Supplemental Information.

RPA, RIP, and RIP-Seq

For RPA, we used a protocol described in a previous publication (Huarte et al., 2010). Briefly, 20 μl M-280 Dynabeads (Life Technologies) was allowed to bind to 300 ng biotin-labeled sense or anti-sense *Apela* overnight. The Dynabeads/RNA complexes were incubated with 400 μl of 2 μg/μl whole-cell lysates at 4°C for 1 hr. Dynabeads were washed three times (5 min each) with RPA buffer (50 mM Tris [pH 7.5], 250 mM KCl, 5 mM EDTA, 0.5 mM DTT, and 1% NP40 plus protease inhibitors and RNase inhibitors). After washes, beads were boiled, the supernatant was run on a 4%–12% NuPAGE gel, and silver staining was performed using the SilverQuest Silver Staining Kit (Life Technologies). Bands were cut out from the gel and sent for protein identification using mass spectrometry.

For RIP, 1 μg hnRNPL Ab was incubated with Protein A-Dynabeads overnight and then incubated with 500 μg total clear lysate in RPA buffer at 4°C for 4 hr. We washed the beads four times with RPA buffer and extracted the total RNA with Trizol. The concentration was measured and 100 ng RNA was sent to the NGSF at CCR, NCI. For data processing, we applied a normalization approach because input and RIP had different averages of all the FPKMs (fragments per kilobase per million). We made an assumption that the majority of the RNAs were not bound by hnRNPL. Therefore, we normalized the FPKM of every transcript to the average of all the transcripts.

ACCESSION NUMBERS

The accession number for the genomic sequence data reported in this paper is GEO: GSE65491. Re-analyzed public datasets were described in Table S5.

SUPPLEMENTAL INFORMATION

Supplemental Information for this article includes seven figures, five tables, and Supplemental Experimental Procedures and can be found with this article online at http://dx.doi.org/10.1016/j.stem.2015.04.002.

AUTHOR CONTRIBUTIONS

M.L. and H.G. conducted the experiments except for confocal microscopy (performed by B.T.), RNA second structure prediction (by J.H. [HHMI] and M.L.), mouse breeding and ESC derivation (by W.D.), cloning (by S.J.), protein identification (by T.W. and M.Z.), and computation and statistical analyses (by J.S. and J.H. [NCI]). J.H. (NCI) designed the project and wrote the manuscript. All authors read the manuscript and approved the submission.

ACKNOWLEDGMENTS

We thank Douglas Lowy for reading the manuscript. This study was funded by the intramural research program and partially funded by the Office of Science and Technology Partnerships at the CCR, the National Cancer Institute (NCI) at the National Institutes of Health (NIH). The computational analyses utilized the high-performance computational capabilities of the Helix Systems at NIH (http://helix.nih.gov).

Received: August 4, 2014
Revised: December 11, 2014
Accepted: April 7, 2015
Published: April 30, 2015

REFERENCES

Berger, S.L. (2007). The complex language of chromatin regulation during transcription. Nature *447*, 407–412.

Cervantes, R.B., Stringer, J.R., Shao, C., Tischfield, J.A., and Stambrook, P.J. (2002). Embryonic stem cells and somatic cells differ in mutation frequency and type. Proc. Natl. Acad. Sci. USA *99*, 3586–3590.

Chaudhury, A., Chander, P., and Howe, P.H. (2010). Heterogeneous nuclear ribonucleoproteins (hnRNPs) in cellular processes: Focus on hnRNP E1's multifunctional regulatory roles. RNA *16*, 1449–1462.

Chen, X., Xu, H., Yuan, P., Fang, F., Huss, M., Vega, V.B., Wong, E., Orlov, Y.L., Zhang, W., Jiang, J., et al. (2008). Integration of external signaling pathways with the core transcriptional network in embryonic stem cells. Cell *133*, 1106–1117.

Chng, S.C., Ho, L., Tian, J., and Reversade, B. (2013). ELABELA: a hormone essential for heart development signals via the apelin receptor. Dev. Cell *27*, 672–680.

Cinghu, S., Yellaboina, S., Freudenberg, J.M., Ghosh, S., Zheng, X., Oldfield, A.J., Lackford, B.L., Zaykin, D.V., Hu, G., and Jothi, R. (2014). Integrative framework for identification of key cell identity genes uncovers determinants of ES cell identity and homeostasis. Proc. Natl. Acad. Sci. USA *111*, E1581–E1590.

Donehower, L.A., Harvey, M., Slagle, B.L., McArthur, M.J., Montgomery, C.A., Jr., Butel, J.S., and Bradley, A. (1992). Mice deficient for p53 are developmentally normal but susceptible to spontaneous tumours. Nature *356*, 215–221.

Dumitru, R., Gama, V., Fagan, B.M., Bower, J.J., Swahari, V., Pevny, L.H., and Deshmukh, M. (2012). Human embryonic stem cells have constitutively active Bax at the Golgi and are primed to undergo rapid apoptosis. Mol. Cell *46*, 573–583.

Goh, A.M., Lim, C.Y., Chiam, P.C., Li, L., Mann, M.B., Mann, K.M., Menendez, S., and Lane, D.P. (2012). Using targeted transgenic reporter mice to study promoter-specific p53 transcriptional activity. Proc. Natl. Acad. Sci. USA *109*, 1685–1690.

(G) Co-IP showing the effect of *Apela* knockdown on the interaction between p53 and hnRNPL: co-IP in mESCs (shLuc, shApela_1, and shApela_2) using p53 Ab followed by W.B. with hnRNPL, p53, and β-actin Abs.
(H) Left, a model of a tri-element negative feedback loop formed by p53, *Apela*, and hnRNPL; right, the well-established negative feedback loop involving p53 and Mdm2 shown as a comparison.
See also Figure S7.

Han, M.K., Song, E.K., Guo, Y., Ou, X., Mantel, C., and Broxmeyer, H.E. (2008). SIRT1 regulates apoptosis and Nanog expression in mouse embryonic stem cells by controlling p53 subcellular localization. Cell Stem Cell *2*, 241–251.

Heintzman, N.D., Stuart, R.K., Hon, G., Fu, Y., Ching, C.W., Hawkins, R.D., Barrera, L.O., Van Calcar, S., Qu, C., Ching, K.A., et al. (2007). Distinct and predictive chromatin signatures of transcriptional promoters and enhancers in the human genome. Nat. Genet. *39*, 311–318.

Hong, Y., and Stambrook, P.J. (2004). Restoration of an absent G1 arrest and protection from apoptosis in embryonic stem cells after ionizing radiation. Proc. Natl. Acad. Sci. USA *101*, 14443–14448.

Huarte, M., Guttman, M., Feldser, D., Garber, M., Koziol, M.J., Kenzelmann-Broz, D., Khalil, A.M., Zuk, O., Amit, I., Rabani, M., et al. (2010). A large intergenic noncoding RNA induced by p53 mediates global gene repression in the p53 response. Cell *142*, 409–419.

Hui, J., Hung, L.H., Heiner, M., Schreiner, S., Neumüller, N., Reither, G., Haas, S.A., and Bindereif, A. (2005). Intronic CA-repeat and CA-rich elements: a new class of regulators of mammalian alternative splicing. EMBO J. *24*, 1988–1998.

Hung, T., Wang, Y., Lin, M.F., Koegel, A.K., Kotake, Y., Grant, G.D., Horlings, H.M., Shah, N., Umbricht, C., Wang, P., et al. (2011). Extensive and coordinated transcription of noncoding RNAs within cell-cycle promoters. Nat. Genet. *43*, 621–629.

Ingolia, N.T., Lareau, L.F., and Weissman, J.S. (2011). Ribosome profiling of mouse embryonic stem cells reveals the complexity and dynamics of mammalian proteomes. Cell *147*, 789–802.

Jones, S.N., Roe, A.E., Donehower, L.A., and Bradley, A. (1995). Rescue of embryonic lethality in Mdm2-deficient mice by absence of p53. Nature *378*, 206–208.

Kagey, M.H., Newman, J.J., Bilodeau, S., Zhan, Y., Orlando, D.A., van Berkum, N.L., Ebmeier, C.C., Goossens, J., Rahl, P.B., Levine, S.S., et al. (2010). Mediator and cohesin connect gene expression and chromatin architecture. Nature *467*, 430–435.

Klattenhoff, C.A., Scheuermann, J.C., Surface, L.E., Bradley, R.K., Fields, P.A., Steinhauser, M.L., Ding, H., Butty, V.L., Torrey, L., Haas, S., et al. (2013). Braveheart, a long noncoding RNA required for cardiovascular lineage commitment. Cell *152*, 570–583.

Kruse, J.P., and Gu, W. (2009). Modes of p53 regulation. Cell *137*, 609–622.

Lee, K.H., Li, M., Michalowski, A.M., Zhang, X., Liao, H., Chen, L., Xu, Y., Wu, X., and Huang, J. (2010). A genomewide study identifies the Wnt signaling pathway as a major target of p53 in murine embryonic stem cells. Proc. Natl. Acad. Sci. USA *107*, 69–74.

Lee, D.F., Su, J., Ang, Y.S., Carvajal-Vergara, X., Mulero-Navarro, S., Pereira, C.F., Gingold, J., Wang, H.L., Zhao, R., Sevilla, A., et al. (2012). Regulation of embryonic and induced pluripotency by aurora kinase-p53 signaling. Cell Stem Cell *11*, 179–194.

Li, M., He, Y., Dubois, W., Wu, X., Shi, J., and Huang, J. (2012). Distinct regulatory mechanisms and functions for p53-activated and p53-repressed DNA damage response genes in embryonic stem cells. Mol. Cell *46*, 30–42.

Lin, T., Chao, C., Saito, S., Mazur, S.J., Murphy, M.E., Appella, E., and Xu, Y. (2005). p53 induces differentiation of mouse embryonic stem cells by suppressing Nanog expression. Nat. Cell Biol. *7*, 165–171.

Liu, J.C., Guan, X., Ryan, J.A., Rivera, A.G., Mock, C., Agrawal, V., Letai, A., Lerou, P.H., and Lahav, G. (2013). High mitochondrial priming sensitizes hESCs to DNA-damage-induced apoptosis. Cell Stem Cell *13*, 483–491.

Montes de Oca Luna, R., Wagner, D.S., and Lozano, G. (1995). Rescue of early embryonic lethality in mdm2-deficient mice by deletion of p53. Nature *378*, 203–206.

Motta-Mena, L.B., Heyd, F., and Lynch, K.W. (2010). Context-dependent regulatory mechanism of the splicing factor hnRNP L. Mol. Cell *37*, 223–234.

Moumen, A., Masterson, P., O'Connor, M.J., and Jackson, S.P. (2005). hnRNP K: an HDM2 target and transcriptional coactivator of p53 in response to DNA damage. Cell *123*, 1065–1078.

Parant, J., Chavez-Reyes, A., Little, N.A., Yan, W., Reinke, V., Jochemsen, A.G., and Lozano, G. (2001). Rescue of embryonic lethality in Mdm4-null mice by loss of Trp53 suggests a nonoverlapping pathway with MDM2 to regulate p53. Nat. Genet. *29*, 92–95.

Pauli, A., Norris, M.L., Valen, E., Chew, G.L., Gagnon, J.A., Zimmerman, S., Mitchell, A., Ma, J., Dubrulle, J., Reyon, D., et al. (2014). Toddler: an embryonic signal that promotes cell movement via Apelin receptors. Science *343*, 1248636.

Rahl, P.B., Lin, C.Y., Seila, A.C., Flynn, R.A., McCuine, S., Burge, C.B., Sharp, P.A., and Young, R.A. (2010). c-Myc regulates transcriptional pause release. Cell *141*, 432–445.

Ray, P.S., Jia, J., Yao, P., Majumder, M., Hatzoglou, M., and Fox, P.L. (2009). A stress-responsive RNA switch regulates VEGFA expression. Nature *457*, 915–919.

Rinn, J.L., Kertesz, M., Wang, J.K., Squazzo, S.L., Xu, X., Brugmann, S.A., Goodnough, L.H., Helms, J.A., Farnham, P.J., Segal, E., and Chang, H.Y. (2007). Functional demarcation of active and silent chromatin domains in human HOX loci by noncoding RNAs. Cell *129*, 1311–1323.

Tsai, M.C., Manor, O., Wan, Y., Mosammaparast, N., Wang, J.K., Lan, F., Shi, Y., Segal, E., and Chang, H.Y. (2010). Long noncoding RNA as modular scaffold of histone modification complexes. Science *329*, 689–693.

Young, R.A. (2011). Control of the embryonic stem cell state. Cell *144*, 940–954.

Zhang, X., He, Y., Lee, K.H., Dubois, W., Li, Z., Wu, X., Kovalchuk, A., Zhang, W., and Huang, J. (2013). Rap2b, a novel p53 target, regulates p53-mediated pro-survival function. Cell Cycle *12*, 1279–1291.